

ANSO Highlight for Agricultural Remote Sensing is a new series dedicated to showcasing cutting-edge remote sensing techniques tailored for agricultural applications. This publication highlights three key contributions of remote sensing to agriculture: crop type classification, crop yield forecasting, and mapping of crop management practices.

Through a collection of valuable case studies, it underscores the pivotal role of remote sensing in delivering operational, efficient, and long-term solutions for agricultural challenges. Furthermore, it calls on multiple stakeholders to leverage the full potential of remote sensing technology to promote sustainable agriculture.

Special Issue

November
2024

Issue.06



Agriculture provides humanity with essential resources such as food, fibers, fuel, and raw materials, which are vital for human well-being. However, the combined challenges of climate change and an ever-growing global population are placing unprecedented pressure on agricultural systems, resulting in food insecurity and potential crises. To address these challenges, it is imperative to adopt sustainable, climate-smart agricultural practices that ensure food security and livelihoods while minimizing agriculture's environmental impact.

For decades, remote sensing has provided timely, repetitive insights into crop conditions throughout the growing season, across various scales, and tailored to the needs of diverse stakeholders. The integration of new remote sensing data, advanced methodologies, and cloud computing infrastructure is now driving a paradigm shift in operational agricultural monitoring, offering new possibilities for addressing agricultural challenges.

Here, three key aspects of agricultural monitoring are highlighted, including:

Crop Type Classification

- 📍 Large Scale Crop mapping
- 📍 Early-season crop mapping and planting area prediction
- 📍 Early-season maize mapping without crop labels
- 📍 Large Scale Orchards mapping

Crop Yield Forecasting

- 📍 ChinaWheatYield30m: an annual winter wheat yield dataset
- 📍 Large-scale yield estimates
- 📍 Estimating yield losses from meteorological disasters

Crop Practices Mapping

- 📍 Global maximum irrigation extent at 30m resolution
- 📍 Irrigation regime mapping for Chinese paddy cropland
- 📍 Global cropping intensity mapping at 30 m resolution
- 📍 Tillage practices mapping across Chinese cropland

Crop Type Classification

1. Large Scale Crop mapping

Detailed maps of crop type information are a prerequisite to mapping farm management and yield outcomes, and to developing strategies for an economically and ecologically sustainable agriculture.

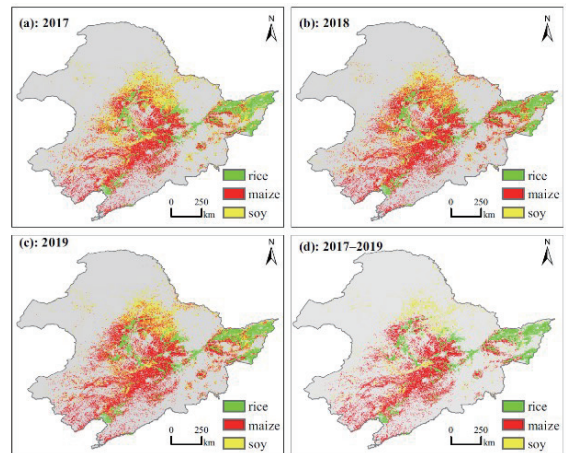
The convergence of advanced Earth Observation (EO), machine learning algorithms, and cloud computing infrastructure now enables the creation of cost-effective, large-scale crop type maps.

The Sentinel-2 satellite constellation (S2), equipped with three red-edge bands and two SWIR bands, captures the crop structural and physiological characteristics. With its 5-day revisit cycle, S2 enables the construction of regular, gap-filled image time series, facilitating the ability to identify different crop types.

Using Northeast China as an example, we demonstrate **a scalable methodology** for generating multi-year, regional-scale crop type maps using Sentinel-2 images (You et al. 2021).

- ④ hierarchical mapping strategy (cropland mapping followed by crop classification)
- ④ agro-climate zone-specific random forest classifiers
- ④ interpolated and smoothed 10-day Sentinel-2 time series data
- ④ optimized features selected from spectral, temporal, and texture feature candidates

The resulting crop type maps have relatively high overall accuracies and agreed well with the statistical data. This is the first effort on regional annual crop mapping in China at the 10-m resolution, which permits assessing the performance of the agricultural subsidy policies and conservation practices (Di et al. 2023).



The crop maps in Northeast China in 2017 (a), 2018 (b), and 2019 (c), and the unchanged rice, maize and soybean during 2017–2019 (d).

Reference

- You, N., Dong, J., Huang, J., Du, G., Zhang, G., He, Y., Yang, T., Di, Y., Xiao, X., 2021. The 10-m crop type maps in Northeast China during 2017–2019. **Sci Data**. 8, 41.
- Di, Y.Y., You, N.S., Dong, J.W., Liao, X.Y., Song, K.S., Fu, P., 2023. Recent soybean subsidy policy did not revitalize but stabilize the soybean planting areas in Northeast China. **Eur. J. Agron**. 147.

2. Early-season crop mapping and planting area prediction

Timely identifying crop types in the early growing season is more valuable for crop insurance, land rental, supply-chain logistics, and food market, compared with the post-harvest mapping efforts.

Challenges will emerge inevitably when dealing with early-season crop mapping:

- Field samples in the current year might be inaccessible for early-season crop mapping.
- Satellite observations in the early season might be insufficient for crop mapping.
- Most crops in the early season might have similar morphology.
- The small plants and weak vegetative signatures in the early season make their spectrum susceptible to background soil conditions.

We employed a **classifier-transfer strategy** to deal with the unavailability of current-year field samples (You and Dong 2020). The Random Forest classifiers were trained based on Sentinel-2 (S2) images and ground samples in the previous year, then were transferred (applied) to the current year for crop type identification and planting area prediction.

Furthermore, we examined the **earliest identifiable timing (EIT)** when a specific crop can be recognized by S2 images. Interestingly, we found different crops exhibit varied EIT in the Northeast China. Specifically, rice could be identified in the late transplanting stage, followed by corn recognizable in the early heading stage and soybean in the early pod setting stage.

This result suggests that we can capture the planting area of rice up to four months before harvest, and for corn and soybean around two months before harvest. Obtaining food supply information 2-4 months in advance is valuable for stakeholders and decision-makers across various sectors.

	Apr			May			Jun			July			Aug			Sep			Oct		
	E	M	L	E	M	L	E	M	L	E	M	L	E	M	L	E	M	L	E	M	L
Rice	1	2	2/3	3	4		5			6	7		8			9/10	10				
Corn				1	2	3	4			5			6	7	8						
Soybean					1	2	3	4					5			6/7					

Location of Earliest identifiable timings (EITs) in crops' calendars. The numbers represented different crop phenological stages. Red numbers emphasized the phenological stage where EIT is located. Red solid boxes labelled the image time series used for early season crop mapping. Paddy rice: 1 – Sowing, 2 – Seeding/Flooding, 3 – Transplanting, 4 – Reviving, 5 – Tilling, 6 – Booting, 7 – Heading, 8 – Milkstage, 9 – Mature and 10 – Harvest; Corn: 1 – Sowing, 2 – Seeding/Three leaves, 3 – Seven leaves, 4 – Stem elongation, 5 – Heading, 6 – Milk, 7 – Mature and 8 – Harvest; Soybean: 1 – Sowing, 2 – Seeding, 3 – The 3rd true leaf, 4 – Flowering, 5 – Pod setting, 6 – Mature and 7 – harvest.

Reference

- You, N., Dong, J., 2020. Examining earliest identifiable timing of crops using all available Sentinel 1/2 imagery and Google Earth Engine. **ISPRS J. Photogramm. Remote Sens.** 161, 109-123.

3. Early-season maize mapping Without crop labels

Existing early-season crop type mapping efforts generally rely on crop labels to train classifiers, limiting the potential applications to new regions lacking crop labels. Crop labels for mapping tasks are often scarce. Even when costly crop labels are available, they are typically limited to small regions. Using machine learning to extrapolate crop type maps beyond the training region often results in poor transferability due to the heterogeneity of agricultural landscapes. Unsupervised methods offer a promising approach to address scenarios lack of crop labels.

To explore the possibility of maize mapping without crop labels, we proposed a Multi-temporal Gaussian Mixture Model (MGMM) to map maize planting areas only using early-season Sentinel-2 images (You et al. 2023). A chlorophyll content relevant proxy, named the Red-edge position (REP), was selected as model input, based on the truth that summer maize tends to show a higher chlorophyll content than other summer crops (e.g., soybean, cotton, peanut, sunflowers, etc.) in the peak season.

The novel **REP-based MGMM (MGMM-REP)** was applied in four diverse areas (Iowa and Georgia in the US, Heilongjiang province (HLJ) in China, and Grand-Est in France). The MGMM-REP could generate maize maps more than two months before harvest with reasonable accuracy. Since MGMM-REP does not rely on crop labels, it had the potential to be transferred to label-scarce maize-cropped regions and contribute to the international commodity trade and food security forecast.

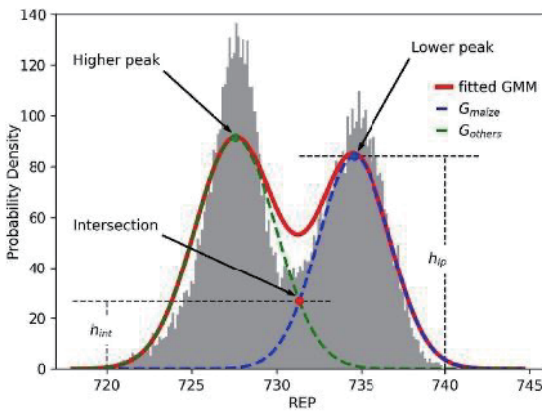
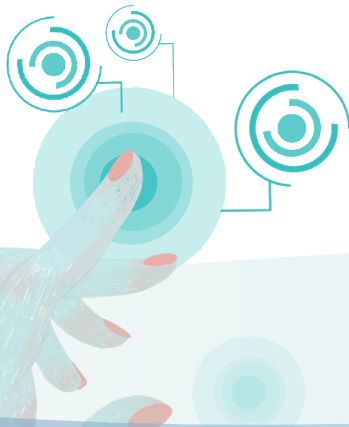


Illustration of the Gaussian Mixture Model (GMM). The histogram was derived from the REP image composited during DOY 190–200 in the year 2020 and in Iowa. The solid red line represented the fitted GMM, and the blue and green dotted lines represented the Gaussian clusters for maize and another summer crop, respectively. The intersection and two peaks of the two Gaussian clusters were labeled.

Reference

- You, N.S., Dong, J.W., Li, J., Huang, J.X., Jin, Z.N., 2023. Rapid early-season maize mapping without crop labels. **Remote Sens. Environ.** 290.

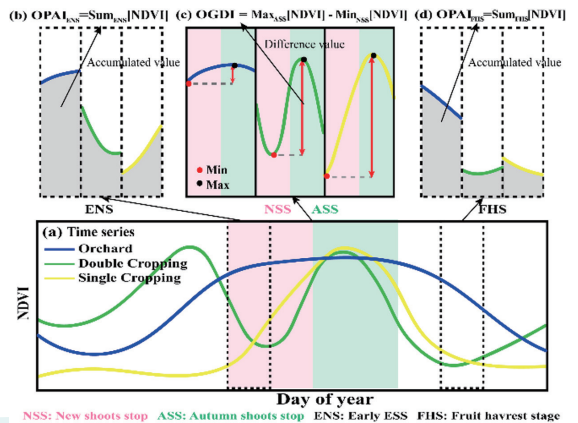


4. Large Scale Orchards mapping

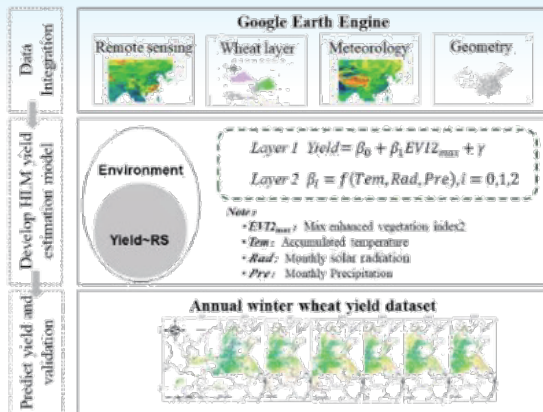
Agroforestry crops such as apples, peaches and pears are horticultural crops, which are an important part of modern agriculture and are of great economic and social importance.

However, existing orchard statistics, survey data, and expert knowledge are often lagging and of low confidence, lacking detailed data on the spatial distribution of orchards. The sparse distribution and indefinite characteristics of orchards compared to grain crops, as well as the large intra-class variance of fruit tree spectra, make large-scale mapping of orchards a major limitation and huge challenge.

Fruit trees possess a unique phenological and greening characteristics that discriminates against grain crops: fruit tree canopies turn green earlier, turn yellow later, and have a long greenness saturation time in annual growth cycles. Therefore, we developed **an orchard mapping index (OMI)** based on the phenology and green-holding characteristics of fruit trees, and automated orchard mapping algorithm (Chen, et al., 2024) using sentinel-2 time-series imagery.

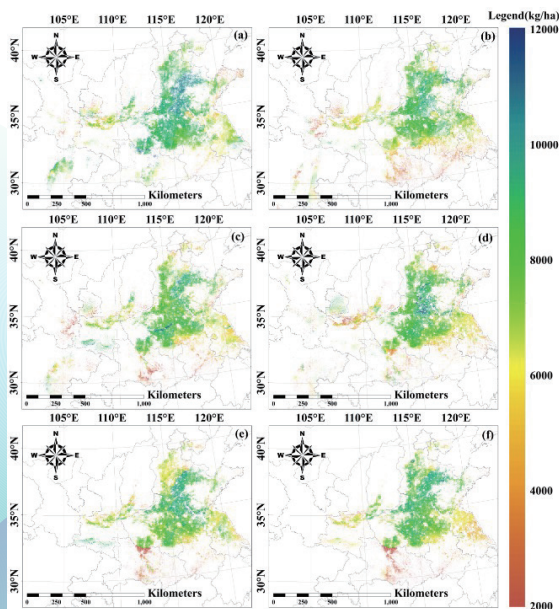


Schematic diagram of the developed orchard mapping index.



Schematic diagram outlining the inputs, major processing steps used and generated outputs.

The results were validated using in situ measurements and census statistics and indicated a stable performance of the HLM based on calibration datasets across China. Such a dataset will provide basic knowledge of detailed wheat yield distribution, which can be applied for many purposes including crop production modeling and regional climate evaluation.



Spatial patterns of annual winter wheat yield for major winter-wheat-producing provinces in China during (a)2016–(f)2021.

Reference

- Zhao, Y., Han, S., Zheng, J., Xue, H., Li, Z., Meng, Y., Li, X., Yang, X., Li, Z., Cai, S., and Yang, G.J., 2022. ChinaWheatYield30m: a 30 m annual winter wheat yield dataset from 2016 to 2021 in China, **Earth Syst. Sci. Data**, 15, 4047–4063.
- Li, Z.H., Taylor J, Yang H., Casa, R., Jin, X.L., Li, Z.H., Song, X.Y, Yang, G.J., 2020. A hierarchical interannual wheat yield and grain protein prediction model using spectral vegetative indices and meteorological data. **Field Crops Res.**, 248: 107711.

2. Large-scale yield estimates

Timely, reliable and large-scale rice production estimates over larger areas are valuable for policy-makers to develop government development plans for food security. Machine Learning (ML) and Deep Learning (DL) techniques as a “black-box” have complex functions and abilities of handling complicated relationships between the predictors and the target variable, have been increasingly employed in agricultural field.

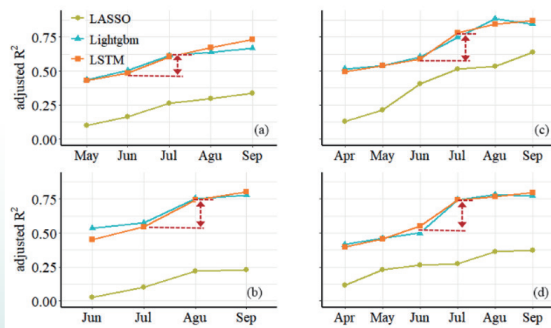
However, high heterogeneity exists in Chinese agricultural systems because of complex crop rotation and intercropping, together with variable topography, climate and field managements across the whole nation. Yield estimation requires huge ground observations and yet often unavailable. Therefore, generating accurate and timely yield estimates remains a big challenge in such tremendous smallholder system.

Using different VIs to investigate the contributions of EVI and SIF to the yield prediction skills (Fig.1), we found ML (RF) and DL (LSTM) obviously outperformed the traditional linear regression models (LASSO) both for the training and testing datasets, with 76% of yield variations for single rice, 80% for early rice, and 84% for late rice.



The R^2 of the three methods using different VIs of inputs for the whole growing season.

To explore early yield prediction, we gradually added the GCVI and S_CI of a specific month to the LightGBM and LSTM models in each agro-ecological zone (Fig.2). The two models showed a similar trajectory with the predicted R^2 increased as more input information was fed into the models. The increases of R^2 varied among stages, independent of methods and zones. LSTM model presented a consistent improvement in predicted R^2 with the progression of time whereas LightGBM was saturated even decreased at the late growing season, highlighting that maize yield could be reasonably estimated approximately one-month in zone I and II and two-month in zone III and IV before maturity.



The performance of the three methods in early season yields prediction. The arrow indicates the month with the largest increase in predicted R^2 . (a) North China spring maize; (b) Huang-Huai-Hai summer maize; (c) Southern maize; (d) Northwest maize.

Reference

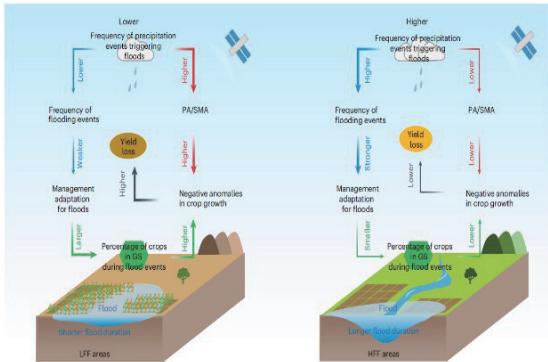
- Cao J., Zhang Z., et al., Integrating multi-source data for rice yield prediction across China using machine learning and deep learning approaches, **Agricultural and Forest Meteorology**, 2021, 297:108275
- Cao J., Zhang Z., Luo Y.C., et al., Wheat yield predictions at a county and field scale with deep learning, machine learning, and google earth engine, **European Journal of Agronomy**, 2021, 123,126204.
- Zhang L.L., Zhang Z., Luo Y.C., et al., Integrating satellite-derived climatic and vegetation indices to predict smallholder maize yield using deep learning, **Agricultural and Forest Meteorology**, 2021, 311:108666

3. Estimating yield losses from meteorological disasters

Natural disasters have long posed a substantial threat to agricultural production worldwide, which is critical yet often overlooked issue of low-frequency floods (LFF) and their significant impact on crop production. Using satellite imagery mapped the spatio-temporal distribution of low-frequency and high-frequency floods (HFF) with remarkable precision, providing a comprehensive understanding of their effects on agriculture. Varying from previous disaster prevention efforts focused on the areas affected by HFFs, however, our study highlighted greater threaten from LFF (Han et al., 2024)

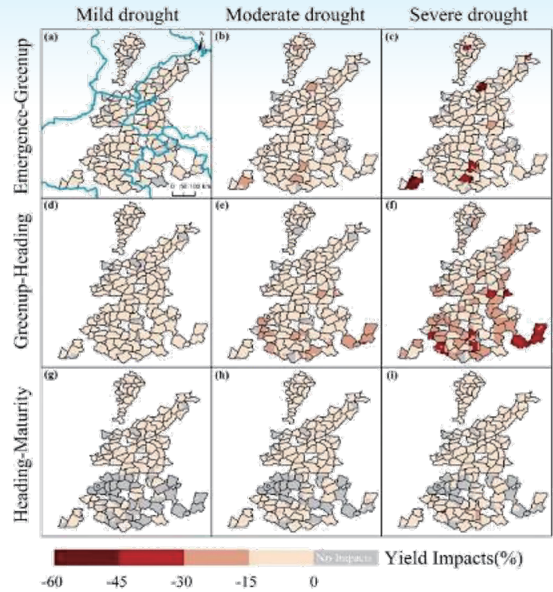
We mapped LFF and HFF over more than 20 years of 3,427 mega-floods globally using satellite imagery at a 250-meter resolution, found LFFs affect a larger proportion of cropland areas (4.7%) compared to HFFs (1.2%), with the greater yield losses of wheat and rice from LFFs compared to HFFs. Furthermore, the expansion of cropland has heightened the risk of flooding exposure (Han et al., 2024). The primary factors contributing to these losses are higher precipitation anomalies, soil moisture anomalies, and greater crop flooding during the critical growing seasons (Fig.3). All such conditions are

particularly detrimental in LFF areas, where crops are not adapted to withstand such extreme events. These findings emphasize the need to study often-overlooked LFF events and offer crucial insights for developing agricultural policies aimed at mitigating flood impacts.



The mechanisms underlying the disparities in crop yield impacts from LFF and HFF.

Similarly, we have estimated accurately other yield losses by extreme climates (drought, heat and cold events) through assimilating crop processes-based models with multi-sources remote sensing data at different spatial scales (Li et al., 2021) (Fig.3). We further designed the climate insurance index based on the related disaster vulnerability curves derived by precisely assessing their related risks (Zhang et al., 2022), with their errors controlled within 1 standard variance.



Wheat yield losses vary by different drought stresses and growing seasons.

Reference

- Han J. Zhang Z , Xu J, et al., Threat of low-frequency high-intensity floods to global cropland and crop yields 2024, **Nature Sustainability**, s41893-024-01375-x#Sec23.
- Li Z.Y., Zhang Z., Zhang L.L., Improving regional wheat drought risk assessment for insurance application by integrating scenario-driven crop model machine learning and satellite data, **Agricultural Systems**, 2021, 191, 103141
- Zhang J., Zhang Z., Wang C. H., et al, Weather index insurance can offset heat-induced rice losses under global warming, **Earth Future**, 2022, 10, e2021EF002534

Crop Practices Mapping

1. Global maximum irrigation extent at 30m resolution

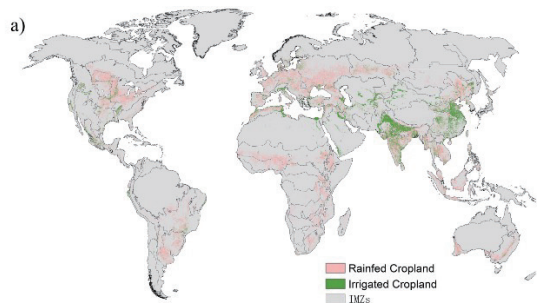
Accurate global irrigation information is essential for managing water scarcity and improving food security. Despite its significance for food security and the global water cycle, irrigation information on a global scale remains highly uncertain. Thus, there is a need to understand the current extent of irrigation to reasonably prioritize irrigation development to ensure food security and the sustainable use of water resources.

The extent of irrigated cropland has been mapped globally using a consistent methodology for a certain time period at a resolution from 250 m to 5 arcmin and at regional scales and national or subnational scales, but the availability of higher resolution irrigation extent datasets is currently limited worldwide and exists mostly at the regional or irrigation district scale. Here, a robust method is proposed using irrigation performance under drought stress as a proxy for crop productivity stabilization and crop water consumption.

For each irrigation mapping zone (IMZ), dry months in the 2017–2019 period and the driest months in the 2010–2019 period were identified over the growing season. The thresholds of the normalized difference vegetation index (NDVI) in the dry months from 2017 to 2019 and the NDVI deviation (NDVIdév) in the driest month were identified to separate irrigated and rainfed cropland with samples. The final threshold from either the NDVI or the NDVIdév of the IMZ was determined with a higher overall accuracy in separating irrigated and non-irrigated areas (Wu, et.al 2023).

The results show that the global maximum irrigation extent (GMIE) at a 30-m resolution was 23.38% of global cropland in 2010–2019 (Tian, et.al 2024), with an overall accuracy of 83.6% globally and significant regional differences in irrigation proportions ranging from 1.1% in western Africa to 100% in Old World deserts among the 110 IMZs and from 0.4% in Belarus to 80.2% in Pakistan and 100% in Egypt among 45 countries. The study quantitatively distinguished annually and inter mittently irrigated regions, which had values of 42% and 58% of global cropland, respectively, by applying indicators.

This method, using the NDVI and NDVIdév thresholds, is simple, concrete and reproducible and better for zones with homogeneous weather conditions. The study offers independent, consistent and comparable information for defining the baseline, tracking changes in irrigation infrastructure, and leading future changes in how stakeholders plan and design irrigation systems.



Global high-resolution irrigated cropland map at 30 m.

Reference

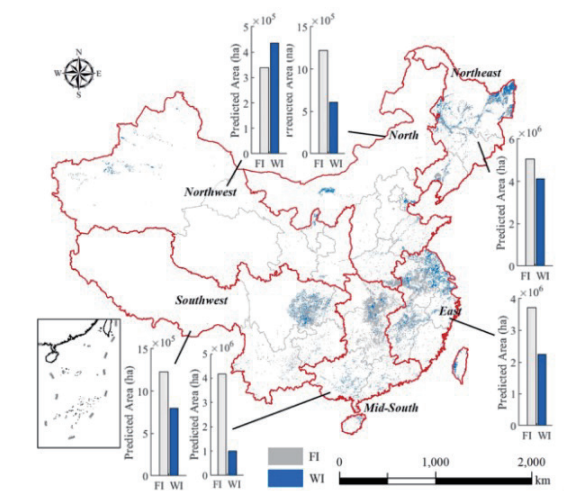
- Tian, F., Wu, B., Zeng, H., Zhang, M., Zhu, W., Yan, N., & Lu, Y. (2024). GMIE: a global maximum irrigation extent and central pivot irrigation system dataset derived through irrigation performance during drought stress and machine learning method. In: **Harvard Dataverse**
- Wu, B., Tian, F., Nabil, M., Bofana, J., Lu, Y., Elnashar, A., Beyene, A.N., Zhang, M., Zeng, H., & Zhu, W. (2023). Mapping global maximum irrigation extent at 30m resolution using the irrigation performances under drought stress. **Global Environmental Change**, 79, 102652

2. Irrigation regime mapping for Chinese paddy cropland

Water-saving irrigation (WI) can save irrigation water, reduce energy consumption, and suppress methane emissions from paddy lands. Classifying WI practices from traditional **flooding irrigation (FI)** can greatly decrease the estimation uncertainty of the total agriculture-associated greenhouse gas emissions.

We began by using seven variables related to irrigation and vegetation cover to create representative WI and FI samples. Additionally, we composited 123 features from optical bands and synthetic aperture radar data from MODIS and Sentinel-1. Then, we trained a random forest model for each province using these samples. Finally, we applied the trained model to generate WI/FI practice maps.

The irrigation regime maps have relatively good overall accuracies and agreed well with the statistical data. This is the first effort on national irrigation regime in China at the 500-m resolution, which provide crucial data support for agricultural emissions reduction (Wang et al., 2024).



Pixel-level water-saving irrigation (WI) frequency, estimated as the number of times each pixel was classified as WI divided by the total number of times that pixel

Reference

- Wang, Y., Tao, F., Chen, Y., Yin, L., 2024. Mapping irrigation regimes in Chinese paddy lands through multi-source data assimilation. **Agr. Water Manag.** 304.

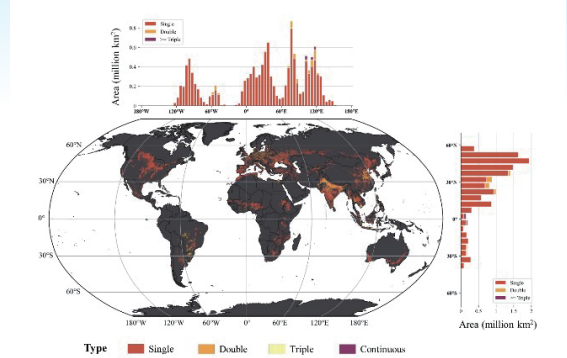
3. Global cropping intensity mapping at 30m resolution

The global distribution of **cropping intensity (CI)** is essential for effective agricultural land use management. Optical remote sensing has enabled extensive CI mapping in a cost-effective manner. Yet, prior studies often used coarse-resolution data, limiting their ability to capture detailed farming practices in varied landscapes.

To bridge this gap, we introduce a 30-m resolution CI mapping framework that reconstructs a time series of Normalised Difference Vegetation Index (NDVI) from multiple satellite images. Using binary crop phenophase profiles, the framework estimates CI on a pixel-by-pixel basis by **detecting valid cropping cycles, distinguishing growth from non-growth periods**. Implemented on the Google Earth Engine (GEE) platform, the algorithm was initially tested across eight diverse regions worldwide, representative of global cropping system diversity.

Comparisons with PhenoCam data in four cropland sites confirm the framework's ability to capture seasonal cropping dynamics. Regionally, validation sample-based accuracies range from 80.0% to 98.9%, with single cropping systems showing more stable estimations compared to multiple cropping systems (Liu et al. 2020). Extrapolated globally, this approach produces the first 30-m resolution global CI map dataset (GCI30), validated by visual interpretation and PhenoCam observations, achieving an overall accuracy of 92.9% (Zhang et al. 2021).

The global average CI from 2016 to 2018 is estimated at 1.05, closely aligning with existing estimates, though with finer spatial detail. Single cropping dominates, covering over 80% of global cropland, while multiple cropping is prevalent in South America and Asia. By providing the first fine-resolution CI map, the GCI30 dataset offers critical insights into global cropping patterns, supporting sustainable agriculture and advancing the understanding of factors driving cropping practices.



Geographical distribution of global CI types during 2016 to 2018 identified by GCI30. The area statistics along latitude and longitude are derived with an interval of five degrees.

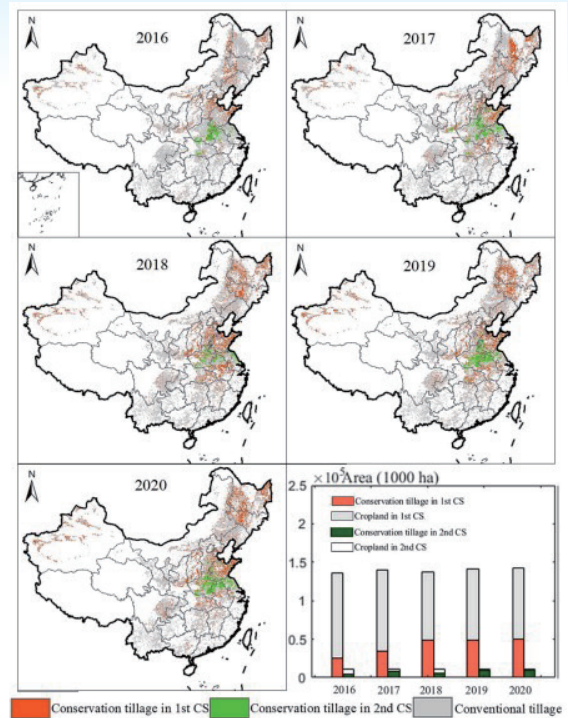
Reference

- Liu, C., Zhang, Q., Tao, S., Qi, J., Ding, M., Guan, Q., Wu, B., Zhang, M., Nabil, M., & Tian, F. (2020). A new framework to map fine resolution cropping intensity across the globe: Algorithm, validation, and implication. **Remote Sensing of Environment**, 251, 112095
- Zhang, M., Wu, B., Zeng, H., He, G., Liu, C., Tao, S., Zhang, Q., Nabil, M., Tian, F., & Bofana, J. (2021). GCI30: a global dataset of 30 m cropping intensity using multisource remote sensing imagery. **Earth System Science Data**, 13, 4799-4817

4. Tillage practices mapping across Chinese cropland

More and more croplands are being converted from conventional tillage to **conservation tillage** in China, which contributes to climate mitigation and yield production. However, where and when conservation tillage practice is implemented at a regional and national scale are not known. Advances in machine learning and Google Earth Engine make it possible to map tillage practices on a large scale.

We first created two ground reference sample pools on tillage practices based on literature and high-resolution maps. Next, we generated Sentinel-2 features during the tillage period using 18 bands related to crop residue ratios. We then trained an optimal random forest (RF) classifier through cross-validation. Finally, we applied this classifier to produce tillage maps for the years 2016 to 2020. The tillage maps have relatively high overall accuracies and agree well with the ground reference samples and statistical data. This is the first effort on national cropland tillage practices in China at the 1-km resolution, which supports the planning of agricultural management and climate change mitigation (Wang et al., 2024).



Spatial patterns and estimated area of tillage methods in two cropping systems from 2016 to 2020.

Reference

- Wang, Y., Tao, F., Chen, Y., Yin, L., 2024. Mapping the spatiotemporal patterns of tillage practices across Chinese croplands with Google Earth Engine. **Comput. Electron. Agric.** 216.